Toxicology Research

PAPER

View Article Online
View Journal | View Issue

Cite this: *Toxicol. Res.*, 2018, **7**, 848

Oxidative stress and mitochondrial impairment mediated apoptotic cell death induced by terpinolene in *Schizosaccharomyces pombe*†

Hizlan H. Agus, * Cemaynur Sarp and Meryem Cemiloglu

Terpinolene is one of the most abundant monoterpenes used as a food supplement or odorant in cosmetics and the pharmaceutical industry. In this study, we aimed to assess apoptotic, oxidative and cytotoxic effects of terpinolene. We used the fission yeast (*Schizosaccharomyces pombe*) as a promising unicellular model organism in molecular toxicology and cell death research, due to its resemblance to mammalian cells at the molecular level. After terpinolene exposure (200–800 mg L^{-1}), the IC_{50} and LC_{50} were calculated as 349.17 mg L^{-1} and 593.87 mg L^{-1}. Cells, stained with acridine orange/ethidium bromide and DAPI, showed apoptotic nuclear morphology, chromatin condensation and fragmentation. 2,7-Dichlorodihydrofluorescein diacetate (DCFDA) fluorescence gradually increased (1.5–2-fold increase) in correlation with increasing concentrations of terpinolene (200–800 mg L^{-1}). Mitochondrial impairment at higher concentrations of terpinolene (400–800 mg L^{-1}) was shown by Rhodamine 123 staining. Real-time PCR experiments showed significant increases (1.5–3-fold) in SOD1 and GPx1 levels ($p < 0.05$) as well as 2–2.5-fold increases ($p < 0.05$) in pro-apoptotic factors, Pca1 and Sprad9. The potential effects of terpinolene on programmed cell death and the underlying mechanisms were clarified in unicellular model fungi, *Schizosaccharomyces pombe*.

Received 4th April 2018,
Accepted 25th April 2018

DOI: 10.1039/c8tx00100f

rsc.li/toxicology-research

1. Introduction

Monoterpenic essential oils (also known as monoterpene hydrocarbons) extracted from glandular trichomes and resin ducts of aromatic and medicinal plants, such as the *Pinaceae* family, are secondary metabolites that play a defensive role against herbivores and some pathogens.[1] Hamamelis water and sage leaf extracts, containing monoterpenes, sesquiterpenes and phenolic acids, are known to display anti-inflammatory and antibacterial activity *in vitro* and *in vivo*.[2–4] Terpinolene, one of monoterpenes used widely as a flavoring additive and odorant, is extracted by fractional distillation from turpentine, which is collected from pine balsam[5] as well as *Citrus*, *Juniperus* and *Myristica* species, or produced by the alcoholic sulfuric acid treatment of pinene.[6]

The potential toxicity of terpinolene has been evaluated *in vivo*[7] and *in vitro*.[8] 0.025% and higher terpinolene concentrations were reported to have a protective role against the oxidation of lipophilic and proteinaceous parts of LDL molecules when terpinolene was incubated with human blood plasma.[9] On the other hand, terpinolene increased total antioxidant capacity and total oxidative stress without a genotoxic effect in both primary rat neurons and N2a neuroblastoma cell lines in a dose dependent manner.[10] Besides, inhibition of cell proliferation *via* down-regulating Akt1 expression in K562 cells even in 50 μg ml^{-1} terpinolene concentration was reported.[11] Given the significance of terpinolene in the future of medicine, cytotoxic, inhibitory and cancer fighting potentials together with the underlying mechanisms should be unraveled. Research for terpinolene toxicity mainly focused on laboratory experiments with rats,[7] some plants,[12] plant pests[13] and plant pathogenic fungus.[1] However, the undefined mechanisms of terpinolene toxicity in model fungi are currently limited.

The fission yeast *Schizosaccharomyces pombe* is one of the most studied unicellular model organisms in molecular toxicology, biochemistry and cell biology.[14–16] In laboratory experiments, the fission yeast constitutes a valuable model organism with its characteristics including short generation time,[17] relatively and easily manipulated small genome (approx. 5000 genes),[18] cell-cycle control[16,19] and mitochondrial biogenesis analogous to mammals,[20,21] and also conserved different programmed cell death (PCD) subroutines.[22] Furthermore, the rapid proliferation of yeast cells with metabolic treatments, resembling the Warburg effect in cancer cells, provides oppor-

Department of Molecular Biology and Genetics, Istanbul Yeni Yuzyil University, Istanbul, Turkey. E-mail: agus_hizlan@yahoo.com.tr; Tel: +90 212 444 50 01

†Electronic supplementary information (ESI) available. See DOI: 10.1039/c8tx00100f

tunities in cancer research.[23,24] Therefore, drug candidates for cancer and other human diseases can be evaluated using yeast cells to understand cytotoxic, apoptotic and genotoxic effects not only for risk assessment, but also for underlying mechanisms that are expected to be deciphered.[25–27]

In this study, the potential cytotoxic effects of terpinolene and underlying mechanisms were investigated in experimental unicellular eukaryotic model *S. pombe*. We aimed to assess the effects of terpinolene on the proliferation index, cell viability and programmed cell death; *i.e.* apoptosis. Besides, oxidative stress, mitochondrial impairment or DNA damage induced by terpinolene were evaluated in molecular levels as accounting mechanisms. The study contributes to both understanding terpinolene cytotoxicity and managing risk assessment for future studies.

2. Materials and methods

2.1 Reagents

Methylene blue was obtained from Merck (Istanbul, Turkey). Components of culture media were from BD Difco (Fisher Scientific, Turkey). Glucose was from Emboy (Istanbul, Turkey). Taq polymerase, SYBR Green I Master Mix and cDNA synthesis kit were from Roche (Elips, Turkey). All other chemicals, terpinolene, arsenic(III) oxide, acridine orange, ethidium bromide, DCFDA (2,7-dichlorodihydrofluorescein diacetate) and Rhodamine 123 were purchased from Sigma (Istanbul, Turkey). NBT (*p*-nitro-blue tetrazolium chloride) and DAPI (4′,6-diamidino-2-phenylindole) were kind gifts from S. Tuncer-Gurbanov (Bilecik SEU) and E. Yoruk (Istanbul YYU).

2.2 Yeast strain, media and growth conditions

S. pombe wild type strain (Sp972h$^-$) was a kind gift from A. T. Sarikaya (Istanbul YYU). Yeast was grown in a standard YEL medium (1% yeast extract, 2% glucose) on a rotary shaker at 150 rpm at 30 °C in all of the experiments. 1×10^6 cells per ml cultures from overnight incubation (14 h) were used for experiments.

2.3 Terpinolene exposure and toxicity testing

Yeast cells from overnight culture ($OD_{600} \approx 1$) in YEL media were washed with 100 mM phosphate buffer (PBS) with pH 7.4, counted under an optical microscope (Karl-Zeiss) and dispensed to conical flasks at a final concentration of 1×10^6 cells per ml. Cells were exposed to a graded concentration of terpinolene (200–3000 mg L^{-1} in Tween-20) for 3 h. All concentrations were lethal for cells except 200 mg L^{-1} exposure. Therefore, the concentration grade was changed to a range of 0–800 mg L^{-1} (solvent control, 200, 400, 600 and 800 mg L^{-1} of terpinolene). Arsenic(III) oxide was used as a positive control for testing apoptosis.[28] Inhibition of proliferation was assessed using a hemocytometer. Cells were suspended in PBS and a sample (100 µl) of the cell suspension was stained with 100 µl methylene blue (0.1 mg ml^{-1} in 2% sodium citrate buffer) for mortality evaluation. After 5 min incubation at room temperature, mortality was examined under a microscope from at least 500 cells in one biological replicate. Dead cells were blue, and viable cells were colorless. The mortality rate was calculated as a ratio of stained cells to total cells.

2.4 Detection of apoptosis by acridine orange/ethidium bromide (AO/EB) and DAPI

Acridine orange/ethidium bromide dual staining was carried out to detect apoptotic morphology. The AO/EB dual staining assay was performed as previously described.[29] After washing with PBS (pH: 7.4), 100 µl of cells were mixed with 5 µl of acridine orange/ethidium bromide solution (60 µg ml^{-1} of AO: 100 µg ml^{-1} of EB, dissolved in PBS). After 5 min incubation at room temperature, cells were washed with PBS and examined under a fluorescence microscope (Karl-Zeiss, Colibri 7) at λ_{ex} = 500 nm and λ_{em} = 530 nm for acridine orange, and λ_{ex} = 510 nm and λ_{em} = 595 nm for ethidium bromide. While acridine orange permeates into the nucleus of all cells and stains green, ethidium bromide is only taken up by dead cells and stains orange-red when membrane integrity is lost. The cell nucleus was also stained with 1 µg ml^{-1} DAPI (4′,6-diamidino-2-phenylindole) to visualize apoptotic DNA fragmentation and chromatin condensation after fixation with 3.7% formaldehyde for 1 h. The staining assay was performed as previously described.[30] Cells were washed with PBS and examined under a fluorescence microscope (Karl-Zeiss, Colibri 7) at λ_{ex} = 358 nm and λ_{em} = 461 nm.

2.5 Intracellular ROS detection by DCFDA staining and colorimetric NBT assay

Intracellular ROS analysis was performed as indicated previously.[31] Cells were incubated with 10 µM DCFDA in culture media for 1 h before harvesting at 30 °C. Cells were washed twice in ice-cold PBS and examined under a fluorescent microscope (Karl-Zeiss, Colibri 7) at λ_{ex} = 495 nm and λ_{em} = 529 nm. Increasing green fluorescence was associated with ROS pro-

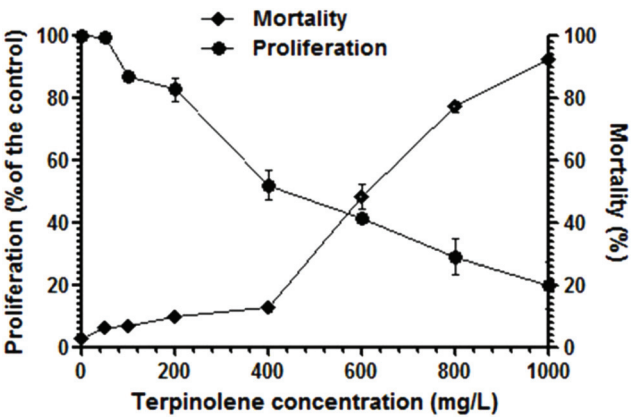

Fig. 1 Cell proliferation and viability after exposure to 0–1000 mg L^{-1} terpinolene solutions for 3 h. Cell proliferation was assessed by a hemocytometer. Mortality of cells was assessed by the Methylene Blue assay. Values are presented as mean ± SEM. Calculations were made from at least five independent biological replica (n = 5).

duction. Intensity analysis was made using a Karl-Zeis Zen 2.3 Blue Edition instrument. The colorimetric NBT assay was performed as previously described.[32] NBT stock solution was prepared at 10 mg ml^{-1} in distilled water. After washing with PBS, cells were incubated with NBT (a final concentration of 0.1%) for 1 h at 1×10^6 cells per ml concentration. The supernatants were removed and the cells were fixed by the addition of 200 μl of absolute methanol and washed twice with 70% methanol, then dried. The final dry pellet was solubilized in 120 μl of 2 M KOH and 140 μl DMSO, and was read at 620 nm in a microplate spectrophotometer (Thermo Scientific, Multiskan Go).

2.6 Detection of mitochondrial transmembrane potential (MTP) by Rhodamine 123 assay

Mitochondria were stained with Rhodamine 123, which is readily sequestered by mitochondria depending on mitochondrial membrane potential, as indicated previously.[33] Cells were suspended in a final concentration of 50 mM sodium citrate (pH 5.0), 2% glucose and 25 μM Rhodamine 123, and incu-

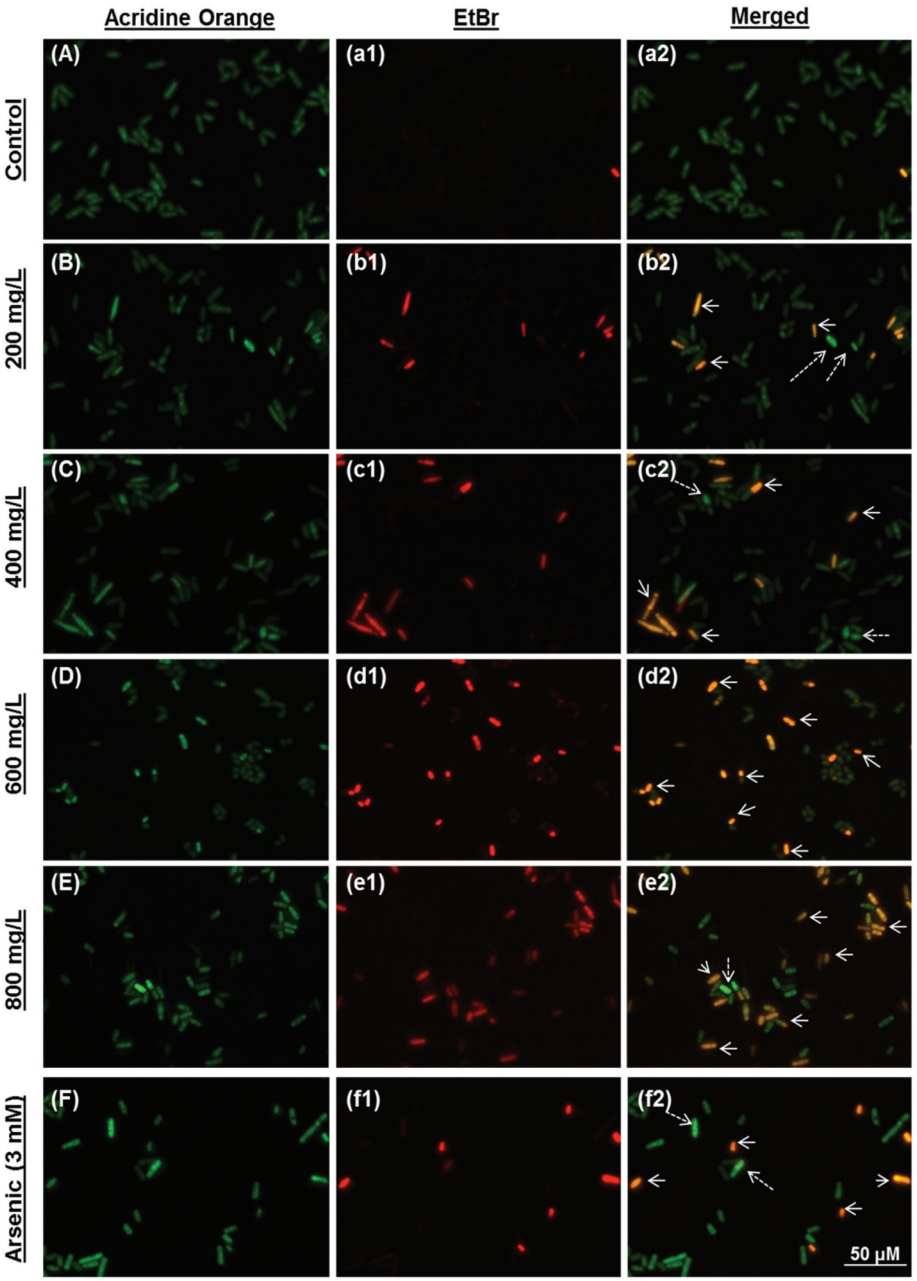

Fig. 2 Apoptosis of *S. pombe* cells was evaluated using acridine orange–ethidium bromide dual staining. Viable, early and late apoptotic/necrotic cells were visualized using a fluorescent microscope after exposure to 0 (A, a1 and a2), 200 (B, b1 and b2), 400 (C, c1 and c2), 600 (D, d1 and d2), 800 (E, e1 and e2) mg L^{-1} terpinolene and 3 mM arsenic(III) (F, f1, f2) solutions. Arsenic(III) was used as a positive control. Arrows: Late apoptotic/necrotic cells; dashed arrows: early apoptotic cells. At least 200 cells were counted in each biological replica (n = 5).

bated 15 min at room temperature. After washing with PBS, cells were visualized by fluorescence microscopy at λ_{ex} = 505 nm and λ_{em} = 534 nm.

2.7 Evaluation of antioxidant enzymes and apoptosis-related genes by mRNA expression assay

The mRNA expression assay for antioxidant enzymes and apoptosis-related genes is described in the ESI.† Gene specific primers were designed using Primer3Plus (Version: 2.3.6) software and declared in Table S1.†

2.8 Statistical analysis

The data were expressed as mean ± standard error of the mean (SEM) and at least three independent experiments were performed. The IC_{50} and LC_{50} values were calculated by the Probit method. Differences between groups were analyzed by One-way ANOVA with Tukey's multiple comparison test using GraphPad Prism (California, USA).

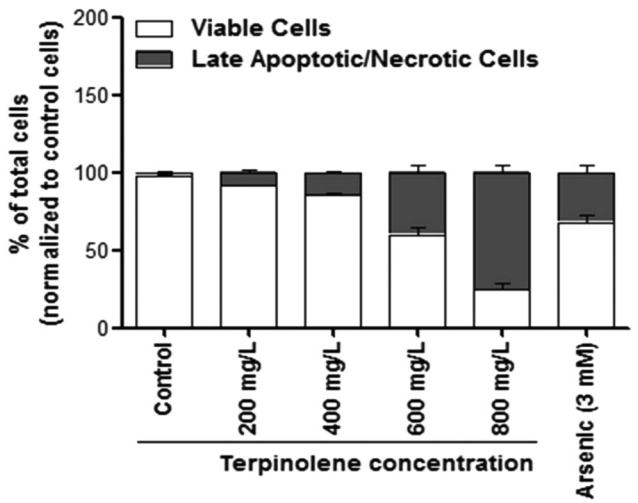

Fig. 3 Percentage of viable and late apoptotic/necrotic cells after exposure to 0–800 mg L^{-1} terpinolene and 3 mM arsenic solutions. At least 200 cells were counted in each biological replica. A small number of early apoptotic cells were ignored. Values are presented as mean ± SEM. Calculations were made from at least five independent biological replicas (n = 5).

3. Results and discussion

3.1 Toxicity testing, cell proliferation and viability

Growth inhibition of cells significantly increased ($p < 0.01$) after exposure to terpinolene at 200–1000 mg L^{-1} (Fig. 1). The IC_{50} value (inhibition concentration 50%) was 349 mg L^{-1}. On the other hand, cell survival notably decreased ($p < 0.01$) gradually after exposure to terpinolene at 200–1000 mg L^{-1}. The LC_{50} value (lethal concentration 50%) was 593 mg L^{-1}. Turkez *et al.* (2015) reported that terpinolene induced cytotoxic cell death even at lower doses (150–200 mg L^{-1}) in human peripheral lymphocyte culture.[34] The difference in mortality rates is probably due to the rigid and relatively impermeable yeast cell wall enforced by crosslinkages between chitin, mannoproteins and β-glucan,[35] although terpinolene, as well as other monoterpenes, is a membrane permeable lipophilic compound.[10] The inhibitory and anti-fungal potentials of terpinolene were found less effective in comparison to other monoterpenes, α-terpineol and 1,8-cineole.[36] Necrosis following changes in cell-membrane fluidity was proposed to explain the anti-fungal action of some monoterpenes.[36] Pontin *et al.*

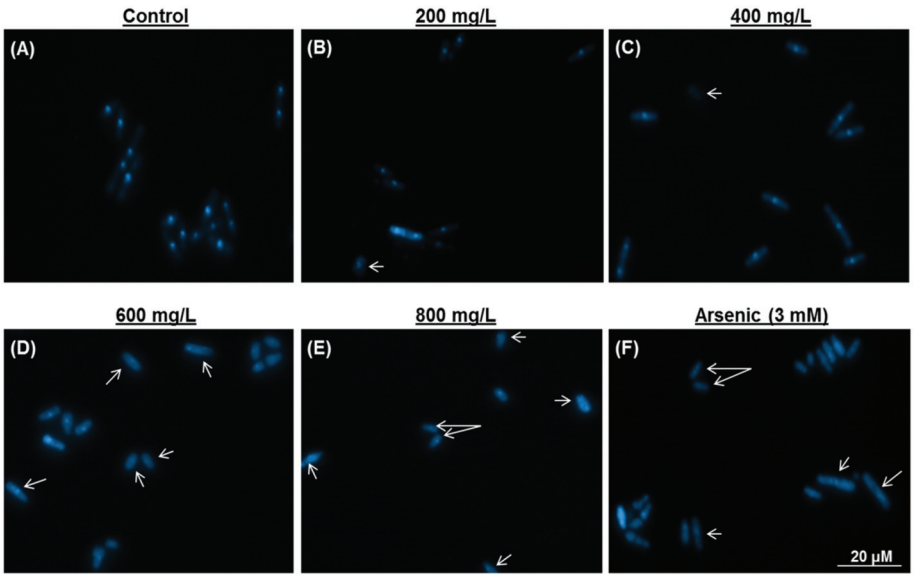

Fig. 4 Nuclear morphology was evaluated using 4,6-diamidino-2-phenylindole (DAPI) staining after exposure to 0 (A), 200 (B), 400 (C), 600 (D), 800 (E) mg L^{-1} terpinolene and 3 mM arsenic(III) (F) solutions. Arsenic(III) was used as a positive control. Arrows: Degraded and fragmented DNA. Images were taken using a fluorescent microscope from at least three independent biological replica (n = 3).

(2015) suggested that alteration in fungal cell membrane permeability was a possible explanation for the anti-fungal activity of terpinolene.[37] In addition, significant increases in lipid peroxidation, ROS levels and total oxidative stress were reported after terpinolene exposure in a variety of species.[10,38] It is well known that excessive ROS production could promote mitochondrial disruption- and oxidative DNA damage-mediated cell death signaling.[39,40]

3.2 Detection of apoptosis

Late apoptotic/necrotic and early apoptotic cells were observed with acridine orange–ethidium bromide dual staining (Fig. 2). Apoptotic and late apoptotic cells were stained bright green and orange-red due to nuclear conformation and cell-membrane status. Apoptotic cells display fragmented and condensed orange-red chromatin, and live cells display a regular green nucleus. Apoptotic cells were indicated by arrows in Fig. 2 (Fig. 2, b2: 200 mg L^{-1}; c2: 400 mg L^{-1}; d2: 600 mg L^{-1}; e2: 800 mg L^{-1} terpinolene and f2: 3 mM arsenic trioxide). As shown in Fig. 3, percentages of the late apoptotic/necrotic cells and viable cells were significantly different in experimental groups (200–800 mg L^{-1}) compared with the control ($p < 0.001$). While apoptotic cells were shown in all concentrations of terpinolene, apoptosis was markedly increased at 600 mg L^{-1} (39.85%), which was close to the mortality rate (47.53%), similar to arsenic induced apoptosis (31.89% at 3 mM). At 800 mg L^{-1}, apoptotic cell death and mortality rates were very similar (75.52% and 77.12%). In order to confirm apoptosis following exposure to terpinolene, cells were fixed with formaldehyde and stained with DAPI. Chromatin condensation and DNA fragmentation, as typical markers of apoptosis, were observed in experimental groups (200–800 mg L^{-1} terpinolene) as shown in Fig. 4. While the nuclei of control cells were seen intact, terpinolene- and arsenic-treated cell nuclei were condensed dot-shaped and crescent-shaped masses, which were previously reported as apoptotic markers.[41–43] Similar results

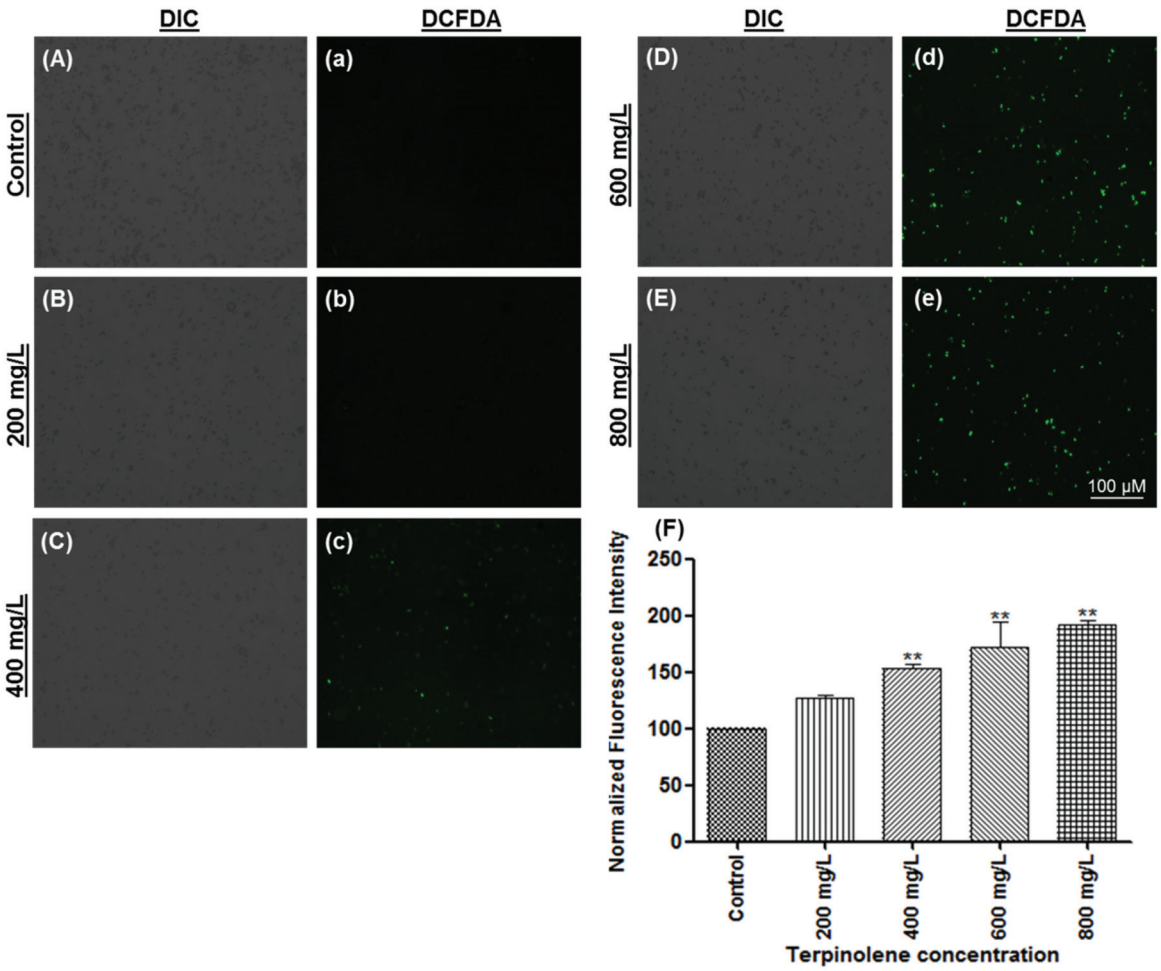

Fig. 5 Measurement of ROS levels using DCFDA (2′,7′-dichlorofluorescin diacetate) staining. ROS generation of cells exposed to 0 (A and a), 200 (B and b), 400 (C and c), 600 (D and d) and 800 (E and e) mg L^{-1} was visualized and measured by a fluorescence microscope. (F) ROS generation of cells exposed to 0–800 mg L^{-1} terpinolene was calculated as normalized fluorescence intensity. Values are presented as mean ± SEM. Statistical analysis was made to compare experimental groups and the control group. Significantly different values are indicated by asterisks (One-way ANOVA, $^{**}p < 0.01$). Images were taken from at least three independent biological replicas ($n = 3$).

were declared by Okumura *et al.*, (2012), who demonstrated that terpinolene induced cell apoptosis in K562 cells.[11]

3.3 Quantification of ROS and antioxidant enzyme mRNA levels

Intracellular ROS levels were shown using the DCFDA fluorescence assay. DCFDA is a membrane permeable dye and reacts with ROS to transform into an oxidized fluorescent form, DCF. As shown in Fig. 5, ROS levels significantly increased ($p < 0.01$) after exposure to terpinolene in a dose-dependent manner (200–800 mg L^{-1}) as indicated by increasing green fluorescence (Fig. 5A and a: control; Fig. 5B and b: 200 mg L^{-1}; Fig. 5C and c: 400 mg L^{-1}; Fig. 5D and d: 600mg L^{-1}; Fig. 5E and e: 800 mg L^{-1}; Fig. 5F: normalized fluorescence intensity). To confirm the results, ROS levels were measured by the NBT assay. The reduction of NBT to insoluble blue formazan is a marker for superoxide generation.[32] Similar to the DCFDA assay, as shown in Fig. 6A, NBT reduction dramatically increased ($p < 0.05$) at 200–600 mg L^{-1} terpinolene exposure analogous with H_2O_2 exposure (0.4 mM). Interestingly, NBT reduction markedly increased more than two-fold ($p < 0.001$) at 800 mg L^{-1} terpinolene exposure similar to arsenic(III) exposure (3 mM). This dramatic increase at 800 mg L^{-1} was consistent with increase in mortality rates (77.21%) and apoptotic cell death (75.52%) at 800 mg L^{-1} (see Fig. 1 and 3). As shown in Fig. 6B and C, SOD1 and GPx1 mRNA levels firstly increased 2–3-fold between 400 and 600 mg L^{-1} terpinolene, however, followed by decreases at 800 mg L^{-1} terpinolene. Upregulation of antioxidant enzyme gene expression generally correlates with increased ROS

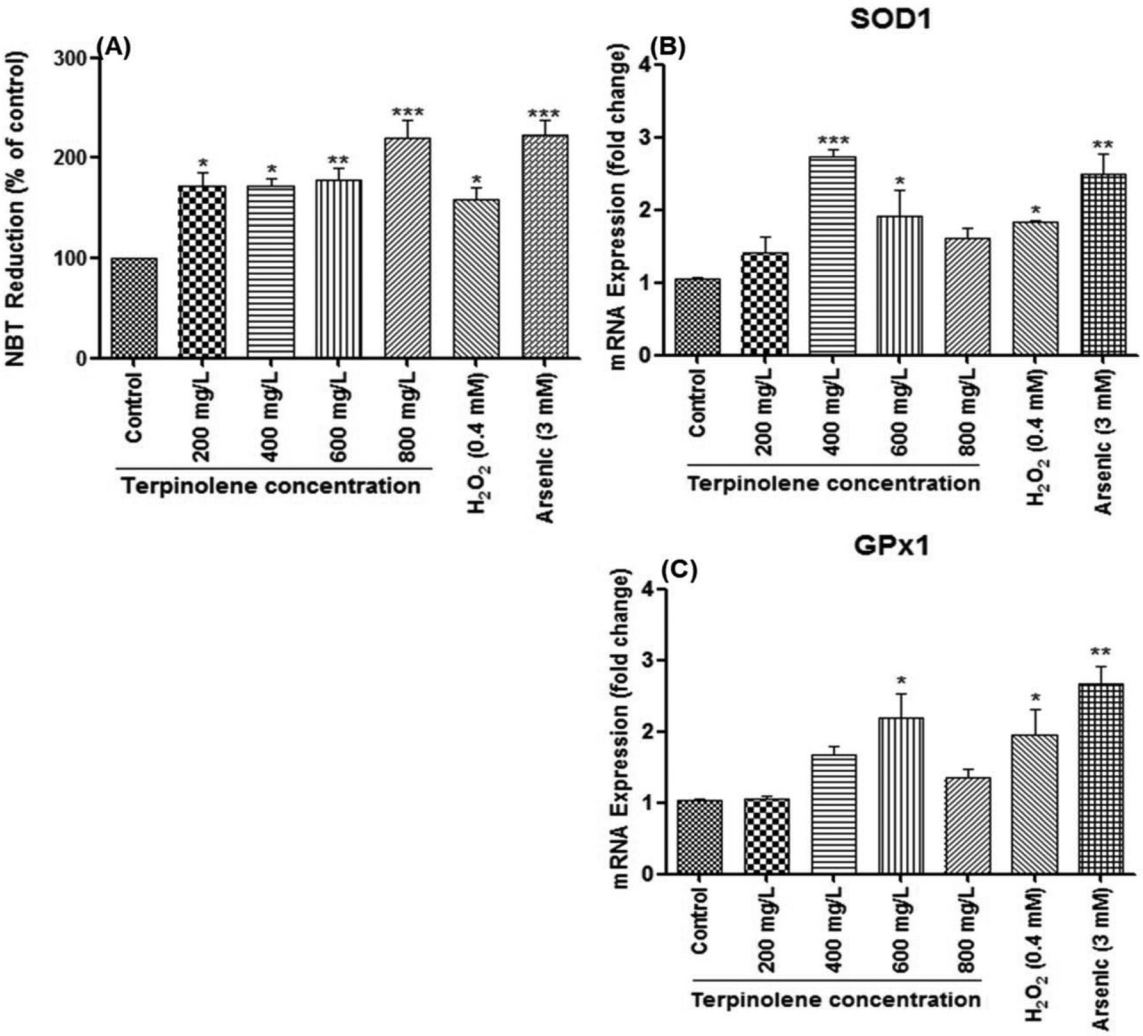

Fig. 6 Cellular ROS levels and gene expression levels of antioxidant enzymes. (A) ROS levels in cells exposed to 0–800 mg L^{-1} terpinolene were measured by the NBT (3,3′-(3,3′-dimethoxy-4,4′-biphenylene)bis[2-(4-nitrophenyl)-5-phenyl-2*H*-tetrazolium chloride) assay. ROS generation of cells was determined as absorbance of reduced NBT at 620 nm in a microplate reader and expressed as normalized NBT reduction compared to the control group. (B and C) mRNA levels of SOD1 and GPx1 in cells exposed to 0–800 mg L^{-1} were measured by RT-PCR. Values are presented as mean ± SEM. Statistical analysis was made to compare experimental groups and the control group. Significantly different values are indicated by asterisks (One-way ANOVA, $*p < 0.05$, $**p < 0.01$, $***p < 0.001$). Values were taken from at least three independent biological replicas ($n = 3$).

levels[44,45] in order to recover the scavenging activity of antioxidant enzymes inhibited by the elevated ROS level.[46] On the other side, recovered gene expression levels at 800 mg L^{-1} may be due to high concentrations of ROS and related increases of mortality rates. Turkez *et al.* (2015) reported a two-fold increase in total oxidative stress levels and mortality rates in cultured human blood cells after exposure to 200 mg L^{-1} terpinolene.[34] Similar results were declared above 200 mg L^{-1} terpinolene in rat brain cells[10] in contrast to other monoterpenes, α-pinene, cineol and myrtenol.[47,48]

3.4 Measuring the mitochondrial transmembrane potential (MTP)

Measuring the mitochondrial transmembrane potential ($\Delta\Psi_m$) is a reliable method to evaluate the vitality of mitochondria.[49] Loss of MTP, generally accepted as a marker for early apoptosis, is monitored using the Rhodamine 123 stain, which is sequestered by intact mitochondria.[50] As shown in Fig. 7, Rhodamine fluorescence was markedly decreased in a dose-dependent manner (200–800 mg L^{-1}) (Fig. 7A, a: control; Fig. 7B, b: 200 mg L^{-1}; Fig. 7C, c: 400 mg L^{-1}; Fig. 7D, d: 600 mg L^{-1} and Fig. 7E, e: 800 mg L^{-1}). Calculated fluorescence intensities dramatically decreased at least 2-fold ($p < 0.01$) at 600 and 800 mg L^{-1} compared with the control (Fig. 7F). Mitochondrial impairment may be due to highly elevated ROS concentrations. It is well known that oxidative stress can result in altered mitochondrial membrane permeability and mitochondrial DNA damage.[51,52] However, mitochondrial dysfunction can stimulate ROS production.[53,54] Our results indicate that apoptosis following terpinolene exposure was related to the dissipation of mitochondrial membrane potential. Similarly, terpinen-4-ol, one of the most known monoterpenes, was shown to induce apoptosis *via* disruption of MTP in human lung cancer cells.[55]

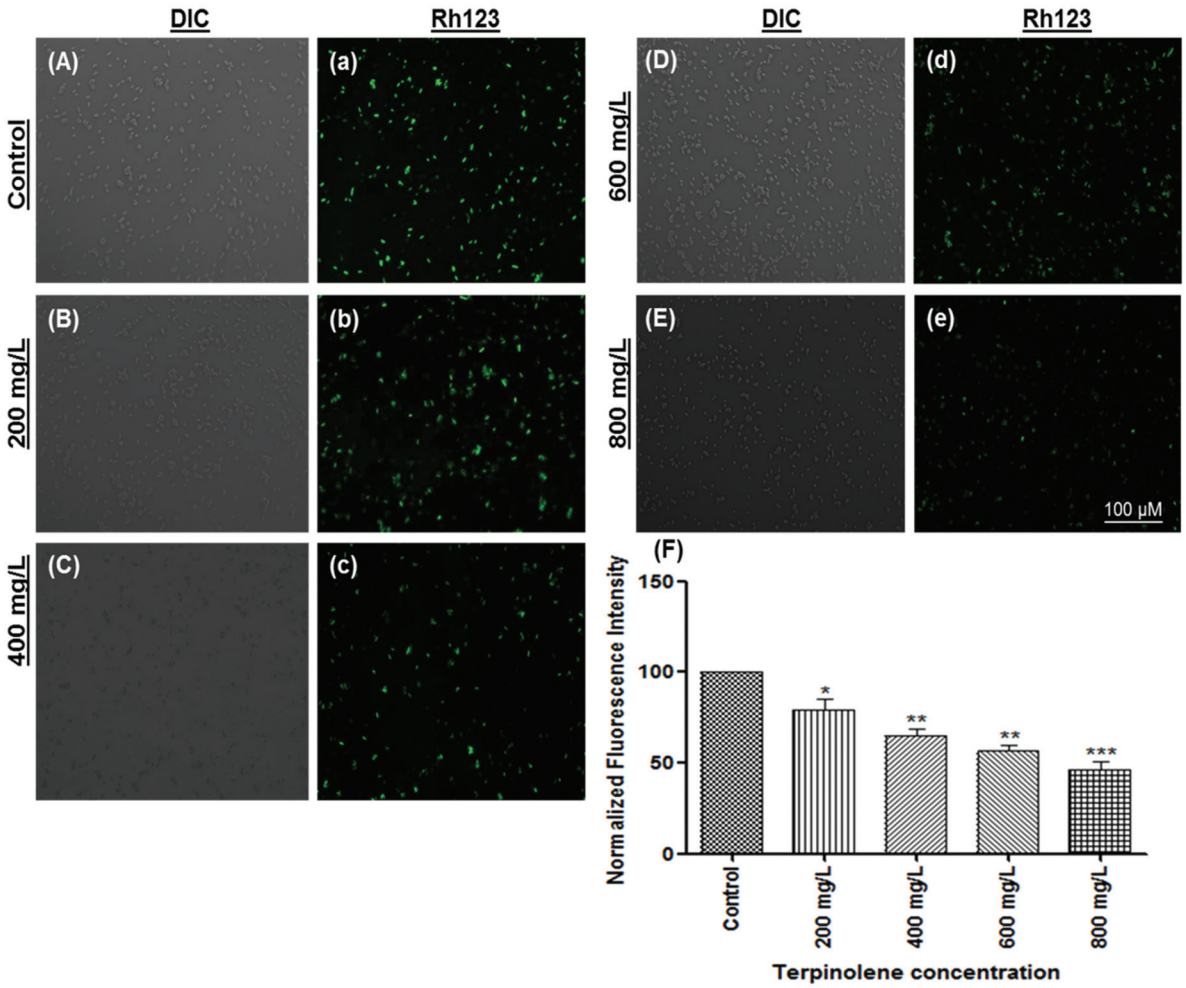

Fig. 7 The mitochondrial transmembrane potential (MTP) of *S. pombe* cells was evaluated using Rhodamine123. The MTP of cells exposed to 0 (A and a), 200 (B and b), 400 (C and c), 600 (D and d) and 800 (E and e) mg L^{-1} terpinolene solutions was visualized and measured by a fluorescence microscope. (F) Dose-dependent decline in the fluorescent intensity of cells exposed to increasing concentrations of terpinolene (0–800 mg L^{-1}) was measured as normalized fluorescence intensity. Values are presented as mean ± SEM. Statistical analysis was made to compare experimental groups and the control group. Significantly different values are indicated by asterisks (One-way ANOVA, *$p < 0.05$, **$p < 0.01$, ***$p < 0.001$). Images were taken from at least three independent biological replicas ($n = 3$).

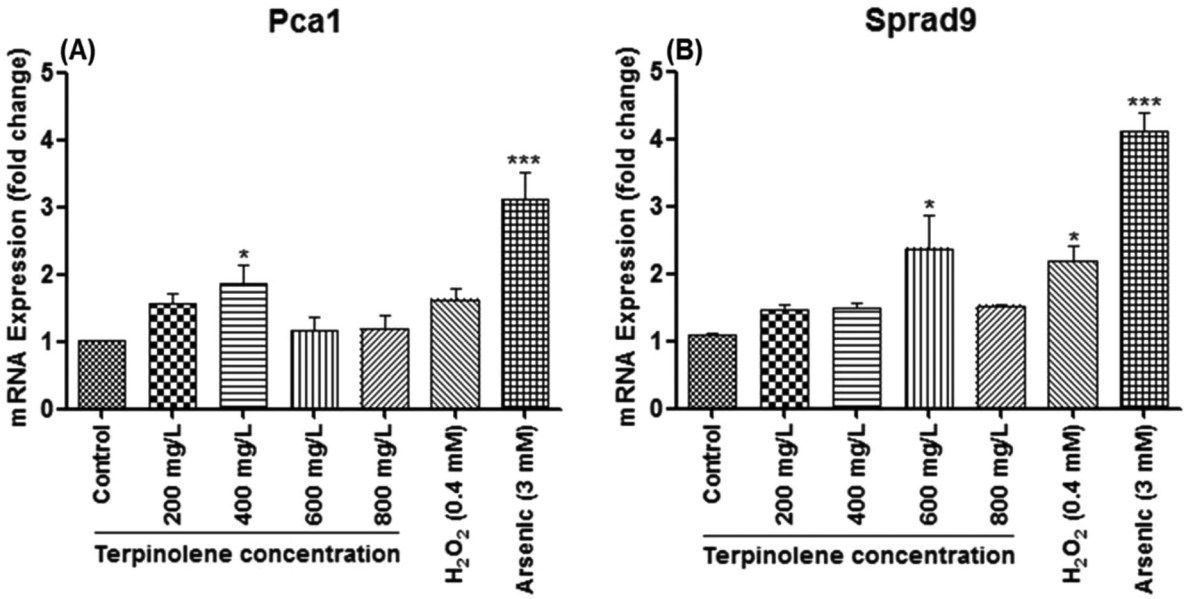

Fig. 8 Apoptosis-related mRNA expression in *S. pombe* cells exposed to 0–800 mg L^{-1} terpinolene. mRNA levels of Pca1 and Sprad9 were measured by RT-PCR. Values are presented as mean ± SEM. Statistical analysis was made to compare experimental groups and the control group. Significantly different values are indicated by asterisks (One-way ANOVA, $*p < 0.05$, $***p < 0.001$). Values were taken from at least three independent biological replicas ($n = 3$).

3.5 Evaluation of apoptotic gene expression

S. pombe caspase 1 (Pca1), homologous to Yca1 of *S. cerevisiae*, is encoded in the *S. pombe* genome and predicted to play a role in apoptosis,[56] whereas Lim *et al.* (2007) suggested that Pca1 can also act as an anti-apoptotic factor in response to chemical stress and relevant toxicity.[57] The precise function of Pca1 in apoptosis still remains unclear.[22] However, as shown in Fig. 8A, Pca1 expression significantly ($p < 0.05$) increased (2-fold) at 400 mg L^{-1} correlating with mortality rates and apoptotic cell death (see Fig. 1 and 3). Interestingly, the obvious decline in Pca1 mRNA levels at 600 and 800 mg L^{-1}, which are close to mRNA levels of untreated cells, may be due to rapid increase in mortality. Another pro-apoptotic gene, Sprad9 (*S. pombe* rad9), which is homologous to human Rad9, functions in DNA damage response.[58] Sprad9 was suggested to have a dual and opposing role in the regulation of apoptosis caused by nutritional and nitrosative stress.[59,60] As illustrated in Fig. 8B, Sprad9 expression dramatically increased ($p < 0.05$) at 600 mg L^{-1} terpinolene and 0.4 mM H_2O_2 concentrations indicating severe DNA damage. The dose-dependent decline of Sprad9 mRNA levels was quite similar to that of Pca1. However, Pca1 and Sprad9 expression were induced up to 4–5-fold in response to 3 mM arsenic trioxide ($p < 0.001$), which reveals the importance of these pro-apoptotic genes in the apoptotic process.

4. Conclusion

In this study, *S. pombe* was assessed as a unicellular eukaryotic model organism to shed light on the potential toxic effects of terpinolene and the underlying mechanism. Cell proliferation and viability significantly decreased after terpinolene exposure. Besides, apoptosis in relation to terpinolene toxicity was shown to be mediated by oxidative stress and reduction of the mitochondrial transmembrane potential. This is the first complete mechanistic study for providing experimental data on terpinolene-induced apoptosis in *S. pombe*. However, experimental data for other programmed cell death mechanisms, autophagy and lipotoxic cell death, are still lacking and warrant further study.

Conflicts of interest

There are no conflicts of interest to declare.

Acknowledgements

This study was supported by the board of trustees of Istanbul Yeni Yuzyil University. We wish to thank Aysegul Topal-Sarikaya, Emre Yoruk and Sinem Tunçer-Gurbanov for consumables and chemicals, Cenk Kig for his advice and for sharing experiences, and Gulsen Uz for providing *S. pombe.*

References

1 A. Farooq, M. I. Choudhary, A. U. Rahman, S. Tahara, K. H. C. Başer and F. Demirci, Detoxification of terpinolene by plant pathogenic fungus Botrytis cinerea, *Z. Naturforsch., C: J. Biosci.*, 2002, **57**, 863–866.

2 R. Dawid-Pać, Medicinal plants used in treatment of inflammatory skin diseases, *Postep Derm. Alergol.*, 2013, **30**, 170–177.
3 D. Trombetta, F. Castelli, M. G. Sarpietro, V. Venuti, M. Cristani, C. Daniele, A. Saija, G. Mazzanti and G. Bisignano, Mechanisms of antibacterial action of three monoterpenes, *Antimicrob. Agents Chemother.*, 2005, **49**, 2474–2478.
4 B. Chueca, R. Pagán and D. García-Gonzalo, Oxygenated monoterpenes citral and carvacrol cause oxidative damage in *Escherichia coli* without the involvement of tricarboxylic acid cycle and Fenton reaction, *Int. J. Food Microbiol.*, 2014, **189**, 126–131.
5 S. Masten and K. E. Haneke, Toxicological Summary For Turpentine [8006-64-2], https://ntp.niehs.nih.gov/ntp/htdocs/chem_background/exsumpdf/turpentine_508.pdf, (accessed 6 November 2017).
6 S. Masten and R. Tice, Toxicological Summary for Terpinolene, http://www.jonnsaromatherapy.com/pdf/Tice_Toxicological_Summary_for_Terpinolene_1999.pdf, (accessed 6 November 2017).
7 U.S. National Library of Medicine, TOXNET Toxicology Data Network, https://toxnet.nlm.nih.gov/cgi-bin/sis/search2/r?dbs+hsdb:@term+@rn+@rel+586-62-9, (accessed 6 November 2017).
8 A. C. Siani, M. F. Ramos, O. Menezes-de-Lima, R. Ribeiro-dos-Santos, E. Fernadez-Ferreira, R. O. Soares, E. C. Rosas, G. S. Susunaga, A. C. Guimarães, M. G. Zoghbi and M. G. Henriques, Evaluation of anti-inflammatory-related activity of essential oils from the leaves and resin of species of *Protium*, *J. Ethnopharmacol.*, 1999, **66**, 57–69.
9 J. Graßmann, S. Hippeli, R. Spitzenberger and E. F. Elstner, The monoterpene terpinolene from the oil of *Pinus mugo* L. in concert with α-tocopherol and β-carotene effectively prevents oxidation of LDL, *Phytomedicine*, 2005, **12**, 416–423.
10 E. Aydin, H. Türkez and Ş. Taşdemir, Anticancer and antioxidant properties of terpinolene in rat brain cells, *Arh. Hig. Rada Toksikol.*, 2013, **64**, 415–424.
11 N. Okumura, H. Yoshida, Y. Nishimura, Y. Kitagishi and S. Matsuda, Terpinolene, a component of herbal sage, downregulates AKT1 expression in K562 cells, *Oncol. Lett.*, 2012, **3**, 321–324.
12 M. F. Russell and I. A. Southwell, Monoterpenoid accumulation in 1,8-cineole, terpinolene and terpinen-4-ol chemotypes of *Melaleuca alternifolia* seedlings, *Phytochemistry*, 2003, **62**, 683–689.
13 J. L. Wang, Y. Li and C. L. Lei, Evaluation of monoterpenes for the control of *Tribolium castaneum* (Herbst) and *Sitophilus zeamaise* Motschulsky, *Nat. Prod. Res.*, 2009, **23**, 1080–1088.
14 J. Laliberté, L. J. Whitson, J. Beaudoin, S. P. Holloway, P. J. Hart and S. Labbé, The *Schizosaccharomyces pombe* Pccs protein functions in both copper trafficking and metal detoxification pathways, *J. Biol. Chem.*, 2004, **279**, 28744–28755.
15 M. Liu, Y. Huang, H. Wen and G. Qiu, Comparing Cell Toxicity of *Schizosaccharomyces pombe* Exposure to Airborne PM2.5 from Beijing and Inert Particle SiO2, *Huanjing Kexue*, 2015, **36**, 3943–3951.
16 I. M. Hagan, A. Grallert and V. Simanis, Analysis of the *Schizosaccharomyces pombe* cell cycle, *Cold Spring Harbor. Protoc.*, 2016, **2016**(9), pdb.top082800.
17 T. Eisenberg, D. Carmona-Gutierrez, S. Büttner, N. Tavernarakis and F. Madeo, Necrosis in yeast, *Apoptosis*, 2010, **15**, 257–268.
18 K. Sajiki, M. Hatanaka, T. Nakamura, K. Takeda, M. Shimanuki, T. Yoshida, Y. Hanyu, T. Hayashi, Y. Nakaseko and M. Yanagida, Genetic control of cellular quiescence in *S. pombe*, *J. Cell Sci.*, 2009, **122** 1418–1429.
19 S. Hartmuth and J. Petersen, Fission yeast Tor1 functions as part of TORC1 to control mitotic entry through the stress MAPK pathway following nutrient stress, *J. Cell Sci.*, 2009, **122**, 1737–1746.
20 B. Schafer, Genetic conservation versus variability in mitochondria: the architecture of the mitochondrial genome in the petite-negative yeast *Schizosaccharomyces pombe*, *Curr. Genet.*, 2003, **43**, 311–326.
21 M. Koyama, W. Nagakura, H. Tanaka, T. Kujirai, Y. Chikashige, T. Haraguchi, Y. Hiraoka and H. Kurumizaka, In vitro reconstitution and biochemical analyses of the *Schizosaccharomyces pombe* nucleosome, *Biochem. Biophys. Res. Commun.*, 2017, **482**, 896–901.
22 S. J. Lin and N. Austriaco, Aging and cell death in the other yeasts, *Schizosaccharomyces pombe* and *Candida albicans*, *FEMS Yeast Res.*, 2014, **14**, 119–135.
23 D. Carmona-Gutierrez, A. Reisenbichler, P. Heimbucher, M. A. Bauer, R. J. Braun, C. Ruckenstuhl, S. Büttner, T. Eisenberg, P. Rockenfeller, K.-U. Fröhlich, G. Kroemer and F. Madeo, Ceramide triggers metacaspase-independent mitochondrial cell death in yeast, *Cell Cycle*, 2011, **10**, 3973–3978.
24 F. Madeo, E. Fröhlich and K. U. Fröhlich, A yeast mutant showing diagnostic markers of early and late apoptosis, *J. Cell Biol.*, 1997, **139**, 729–734.
25 K. Takeda, A. Mori and M. Yanagida, Identification of genes affecting the toxicity of anti-cancer drug bortezomib by genome-wide screening in *S. pombe*, *PLoS One*, 2011, **6**, e22021.
26 D. Villahermosa and O. Fleck, Identification of genes affecting the toxicity of anti-cancer drug bortezomib by genome-wide screening in *S. pombe*, *Sci. Rep.*, 2017, **7**, 7225.
27 W. K. Eng, L. Faucette, R. K. Johnson and R. Sternglanz, Evidence that DNA topoisomerase I is necessary for the cytotoxic effects of camptothecin, *Mol. Pharmacol.*, 1988, **34**, 755–760.
28 L. Du, Y. Yu, J. Chen, Y. Liu, Y. Xia, Q. Chen and X. Liu, Arsenic induces caspase-and mitochondria-mediated apoptosis in *Saccharomyces cerevisiae*, *FEMS Yeast Res.*, 2007, **7**, 860–865.

29 S. Pajaniradje, K. Mohankumar, R. Pamidimukkala, S. Subramanian and R. Rajagopalan, Antiproliferative and apoptotic effects of *Sesbania grandiflora* leaves in human cancer cells, *Biomed. Res. Int.*, 2014, **2014**, 474953.

30 B. Chazotte, Labeling nuclear DNA using DAPI, *Cold Spring Harbor Protoc.*, 2011, **2011**(1), pdb.prot5556.

31 G. K. Azad, V. Singh, P. Mandal, P. Singh, U. Golla, S. Baranwal, S. Chauhan and R. S. Tomar, Ebselen induces reactive oxygen species (ROS)-mediated cytotoxicity in *Saccharomyces cerevisiae* with inhibition of glutamate dehydrogenase being a target, *FEBS Open Biol.*, 2014, **4**, 77–89.

32 M. Muñoz, R. Cedeño, J. Rodríguez, W. P. W. Van Der Knaap, E. Mialhe and E. Bachère, Measurement of reactive oxygen intermediate production in haemocytes of the penaeid shrimp, *Penaeus vannamei*, *Aquaculture*, 2000, **191**, 89–107.

33 M. Kwolek-Mirek and R. Zadrag-Tecza, Comparison of methods used for assessing the viability and vitality of yeast cells, *FEMS Yeast Res.*, 2014, **14**, 1068–1079.

34 H. Turkez, E. Aydın, F. Geyikoglu and D. Cetin, Genotoxic and oxidative damage potentials in human lymphocytes after exposure to terpinolene in vitro, *Cytotechnology*, 2015, **67**, 409–418.

35 B. Aguilar-Uscanga and J. M. Franç, A study of the yeast cell wall composition and structure in response to growth conditions and mode of cultivation, *Lett. Appl. Microbiol.*, 2003, **37**, 268–274.

36 D. Yu, J. Wang, X. Shao, F. Xu, H. Wang and C. X. Shao, Antifungal modes of action of tea tree oil and its two characteristic components against *Botrytis cinerea*, *J. Appl. Microbiol.*, 2015, **119**, 1253–1262.

37 M. Pontin, R. Bottini, J. L. Burba and P. Piccoli, *Allium sativum* produces terpenes with fungistatic properties in response to infection with *Sclerotium cepivorum*, *Phytochemistry*, 2015, **115**, 152–160.

38 R. M. Montanari, L. C. A. Barbosa, A. J. Demuner, C. J. Silva, N. J. Andrade, F. M. D. Ismail and M. C. A. Barbosa, Exposure to Anacardiaceae volatile oils and their constituents induces lipid peroxidation within food-borne bacteria cells, *Molecules*, 2012, **17**, 9728–9740.

39 C. Zhang, S.-H. Lai, H.-H. Yang, D.-G. Xing, C.-C. Zeng, B. Tang, D. Wan and Y.-J. Liu, Photoinduced ROS regulation of apoptosis and mechanism studies of iridium(III) complex against SGC-7901 cells, *RSC Adv.*, 2017, **7**, 17752–17762.

40 X. Xiong, L. Gan, Y. Liu, C. Zhang, T. Yong, Z. Wang, H. Xu and X. Yang, Selective killing of hepatocellular carcinoma HepG2 cells by three-dimensional nanographene nanoparticles based on triptycene, *Nanoscale*, 2015, **7**, 5217–5229.

41 N. Mutoh, S. Kitajima and S. Ichihara, Apoptotic cell death in the fission yeast Schizosaccharomyces pombe induced by valproic acid and its extreme susceptibility to pH change, *Biosci., Biotechnol., Biochem.*, 2011, **75**, 1113–1118.

42 A. J. Munoz, K. Wanichthanarak, E. Meza and D. Petranovic, Systems biology of yeast cell death, *FEMS Yeast Res.*, 2012, **12**, 249–265.

43 S. Salucci, S. Burattini, E. Falcieri and P. Gobbi, Three-dimensional apoptotic nuclear behavior analyzed by means of Field Emission in Lens Scanning Electron Microscope, *Eur. J. Histochem.*, 2015, **59**, 2539.

44 W. Li, L. Chen, Y. Su, H. Yin, Y. Pang and Z. Zhuang, 1,2-Dichloroethane induced nephrotoxicity through ROS mediated apoptosis in vitro and in vivo, *Toxicol. Res.*, 2015, **4**, 1389–1399.

45 S. Zhu, F. Luo, B. Zhu and G.-X. Wang, Mitochondrial impairment and oxidative stress mediated apoptosis induced by α-Fe_2O_3 nanoparticles in *Saccharomyces cerevisiae*, *Toxicol. Res.*, 2017, **6**, 719–728.

46 D. Schnabel, E. Salas-Vidal, V. Narváez, M. del Rayo Sánchez-Carbente, D. Hernández-García, R. Cuervo and L. Covarrubias, Expression and regulation of antioxidant enzymes in the developing limb support a function of ROS in interdigital cell death, *Dev. Biol.*, 2006, **291**, 291–299.

47 M. Porres-Martínez, E. González-Burgos, M. E. Carretero and M. P. Gómez-Serranillos, In vitro neuroprotective potential of the monoterpenes α-pinene and 1,8-cineole against H_2O_2-induced oxidative stress in PC12 cells, *Z. Naturforsch., C: J. Biosci.*, 2016, **71**, 191–199.

48 B. S. Gomes, B. P. S. Neto, E. M. Lopes, F. V. M. Cunha, A. R. Araújo, C. W. S. Wanderley, D. V. T. Wong, R. C. P. L. Júnior, R. A. Ribeiro, D. P. Sousa, J. Venes R Medeiros, R. C. M. Oliveira and F. A. Oliveira, Anti-inflammatory effect of the monoterpene myrtenol is dependent on the direct modulation of neutrophil migration and oxidative stress, *Chem.-Biol. Interact.*, 2017, **273**, 73–81.

49 L. D. Zorova, V. A. Popkov, E. Y. Plotnikov, D. N. Silachev, I. B. Pevzner, S. S. Jankauskas, V. A. Babenko, S. D. Zorov, A. V. Balakireva, M. Juhaszova, S. J. Sollott and D. B. Zorov, Mitochondrial membrane potential, *Anal. Biochem.*, 2017, S0003-2697(17)30293-2, DOI: 10.1016/j.ab.2017.07.009 [Epub ahead of print].

50 A. Baracca, G. Sgarbi, G. Solaini and G. Lenaz, Rhodamine 123 as a probe of mitochondrial membrane potential: Evaluation of proton flux through F(0) during ATP synthesis, *Biochim. Biophys. Acta*, 2003, **1606**, 137–146.

51 C. Guo, L. Sun, X. Chen and D. Zhang, Oxidative stress, mitochondrial damage and neurodegenerative diseases, *Neural Regener Res.*, 2013, **8**, 2003–2014.

52 A. H. Bhat, K. B. Dar, S. Anees, M. A. Zargar, A. Masood, M. A. Sofi and S. A. Ganie, Oxidative stress, mitochondrial dysfunction and neurodegenerative diseases; a mechanistic insight, *Biomed. Pharmacother.*, 2015, **74**, 101–110.

53 A. Zuin, N. Gabrielli, I. A. Calvo, S. García-Santamarina, K.-L. Hoe, D. U. Kim, H.-O. Park, J. Hayles, J. Ayté and E. Hidalgo, Mitochondrial dysfunction increases oxidative stress and decreases chronological life span in fission yeast, *PLoS One*, 2008, **3**, e2842.

54 J. Li, X. Liu, Y. Zhang, F. Tian, G. Zhao, Q. Yu, F. Jiang and Y. Liu, Toxicity of nano zinc oxide to mitochondria, *Toxicol. Res.*, 2012, **1**, 137.

55 C.-S. Wu, Y.-J. Chen, J. J. W. Chen, J.-J. Shieh, C.-H. Huang, P.-S. Lin, G.-C. Chang, J.-T. Chang and C.-C. Lin, Terpinen-4-ol Induces Apoptosis in Human Nonsmall Cell Lung Cancer In Vitro and In Vivo, *Evid. Based Complement. Altern. Med.*, 2012, **2012**, 818261.

56 C. P. Low and H. Yang, Programmed cell death in fission yeast *Schizosaccharomyces pombe*, *Biochim. Biophys. Acta, Mol. Cell Res.*, 2008, **1783**, 1335–1349.

57 H.-W. Lim, S.-J. Kim, E.-H. Park and C.-J. Lim, Overexpression of a metacaspase gene stimulates cell growth and stress response in *Schizosaccharomyces pombe*, *Can. J. Microbiol.*, 2007, **53**, 1016–1023.

58 T. Wakida, M. Ikura, K. Kuriya, S. Ito, Y. Shiroiwa, T. Habu, T. Kawamoto, K. Okumura, T. Ikura and K. Furuya, The CDK-PLK1 axis targets the DNA damage checkpoint sensor protein RAD9 to promote cell proliferation and tolerance to genotoxic stress, *eLife*, 2017, **6**, e29953.

59 M.-H. Kang, E.-H. Park and C.-J. Lim, Protective role and regulation of Rad9 from the fission yeast *Schizosaccharomyces pombe*, *FEMS Microbiol. Lett.*, 2007, **275**, 270–277.

60 C. P. Low, G. Shui, L. P. Liew, S. Buttner, F. Madeo, I. W. Dawes, M. R. Wenk and H. Yang, Caspase-dependent and -independent lipotoxic cell-death pathways in fission yeast, *J. Cell Sci.*, 2008, **121**, 2671–2684.

